

PNNL-34162

Understanding Biases in Sample Preparation Techniques for Coupled Scanning Electron Microscopy and MAMA PuO₂ Morphological Analysis

March 2023

Jason Lonergan Kyle Makovsky Vitaliy Goncharov Michaella Swinhart Luke Sweet Edgar Buck Richard Clark David Meier



DISCLAIMER

This report was prepared as an account of work sponsored by an agency of the United States Government. Neither the United States Government nor any agency thereof, nor Battelle Memorial Institute, nor any of their employees, makes any warranty, express or implied, or assumes any legal liability or responsibility for the accuracy, completeness, or usefulness of any information, apparatus, product, or process disclosed, or represents that its use would not infringe privately owned rights. Reference herein to any specific commercial product, process, or service by trade name, trademark, manufacturer, or otherwise does not necessarily constitute or imply its endorsement, recommendation, or favoring by the United States Government or any agency thereof, or Battelle Memorial Institute. The views and opinions of authors expressed herein do not necessarily state or reflect those of the United States Government or any agency thereof.

PACIFIC NORTHWEST NATIONAL LABORATORY

operated by

BATTELLE

for the

UNITED STATES DEPARTMENT OF ENERGY

under Contract DE-AC05-76RL01830

Printed in the United States of America

Available to DOE and DOE contractors from the Office of Scientific and Technical Information, P.O. Box 62, Oak Ridge, TN 37831-0062

www.osti.gov ph: (865) 576-8401 fox: (865) 576-5728 email: reports@osti.gov

Available to the public from the National Technical Information Service 5301 Shawnee Rd., Alexandria, VA 22312 ph: (800) 553-NTIS (6847) or (703) 605-6000

email: info@ntis.gov
Online ordering: http://www.ntis.gov

Understanding Biases in Sample Preparation Techniques for Coupled Scanning Electron Microscopy and MAMA PuO₂ Morphological Analysis

March 2023

Jason Lonergan Kyle Makovsky Vitaliy Goncharov Michaella Swinhart Luke Sweet Edgar Buck Richard Clark David Meier

Prepared for the U.S. Department of Energy under Contract DE-AC05-76RL01830

Pacific Northwest National Laboratory Richland, Washington 99354

Abstract

In this project, the scanning electron microscopy (SEM) sampling method used during the statistical design study (SDS) was investigated to determine if any sampling biases were present in the analyzed data. Using standard particle size distribution powders from the National Institute of Standards and Technology (NIST 1984 standard reference material) with the origin wet dispersion method, it was determined that a bias to smaller particles was present. This was supported by theoretical calculations using Stokes' law to determine the settling rate of spherical particles of roughly the same size and mass as those found in the SDS.

Based on the theoretical calculations, it was determined that the settling rate for each of the 76 powder sets in the SDS could be unique based on specific particle shape and mass distributions, making a universal correction factor/formula not applicable. Therefore, priority shifted to developing an improved wet dispersion method that significantly reduced the particle settling rate for all particle size and shapes. This was achieved by replacing the original solvent (isopropyl alcohol) with a heavy liquid (lithium heteropolytungstates), which dramatically slowed the settling rate and allowed for the capture of a suitable homogeneous aliquot. SEM imaging and Morphological Analysis for Material Attribution (MAMA) software analysis were conducted on the NIST standard, and the SEM/MAMA data were compared to data captured by a dynamic image analysis particle size analyzer. The resulting data confirmed that the new wet dispersion method does indeed deliver an improved representative aliquot to the SEM stub. For instance, in the NIST certificate, the average particle size is ~17.1 µm ± 2.2 µm with a normal distribution. The initial wet dispersion method resulted in a drastically reduced average particle size of 6.1 µm in addition to a non-representative heavy bi-modal distribution whereas the improved LST wet dispersion method resulting in an average particle size that was much closer to the NIST certificate (12.7 µm) with a similar normal distribution.

Although the improved method was still short of the NIST certificate average, atomic force microscopy analysis determined that the resulting ~20-25% reduction in size was due to particles sinking into the carbon sticky tape used for SEM imaging. It is believed that that this bias can be calibrated in a much more predicable manner than the original settling rate bias. In addition, the matching normal distribution curves between the NIST certificate and the heavy liquid method indicate a much-improved representative aliquot has been sampled and imaged. A surrogate CeO₂ powder was used to reflect PuO₂ more accurately and to aid in implementing radiological controls and shielding. The resulting data sets from the SEM/MAMA method and the particle size analyzer give almost identical average particle sizes and particle distribution statistics. Future work will re-analyze several select runs from the SDS to determine if morphological signatures can be found with the improved sampling method.

Abstract

Acronyms and Abbreviations

Al aluminum

AFM atomic force microscopy
BSE backscattered electron

Ci curie

DIA dynamic image analysis/analyzer

DPM dose per minute FEG field emission gun

HCA high-contamination area

IPA isopropyl alcohol

LANL Los Alamos National Laboratory
LST lithium heteropolytungstates

μm micrometer/microns

MAMA Morphological Analysis for Material Attribution
NIST National Institute of Standards and Technology

PNNL Pacific Northwest National Laboratory

PSA particle size analysis/analyzer

REM roentgen equivalent man
RPM revolutions per minute
SDS statistical design study
SE secondary electron

SEM scanning electron microscope/microscopy

SRM standard reference material

Contents

Abstra	act			ii
Acron	yms ar	ıd Abbrev	viations	iii
1.0	Introd	luction		1
	1.1	Statisti	cal Design Study	1
	1.2	Morpho	ological Particle Analysis	1
2.0	Expe	rimental N	Methods	3
	2.1	Dry Pa	rticle Sampling	3
	2.2	Wet Pa	article Sampling	3
	2.3	Heavy	Liquid Particle Sampling	4
	2.4	SEM		5
	2.5	MAMA		5
	2.6	Dynam	ic Image Analysis	5
3.0	SEM	& MAMA		6
	3.1	Dry Sa	mpling	6
		3.1.1	NIST 1984	6
	3.2	Wet Sa	ampling	8
		3.2.1	NIST 1984	8
	3.3	Heavy	Liquid Wet Sampling	10
		3.3.1	NIST 1984	10
		3.3.2	CeO ₂	16
4.0	Partic	le Size A	nalyzer	18
	4.1	Calibra	tion	18
5.0	Atom	ic Force I	Microscopy	21
6.0	Mente	orship an	d Expertise Development	23
7.0	Futur	e Work		24
8.0	Sumr	nary		25
9.0	Refer	ences		27

Figures

Figure 1.	Images comparing the settling behavior of the heavy liquid (left) and the IPA (right) after (a) 10 sec and (b) 60 sec from removal of the vortex mixer. It's clear the heavy liquid (LST) has a much slower settling rate than the IPA	4
Figure 2.	Typical SEM image from LANL 2016 round robin study using NIST SRM 1984.	6
Figure 3.	Histogram showing the particle size distribution found within the images captured for the LANL 2016 round robin study. The average particle size was found to be 12.22 µm after analyzing over 3,000 individual particles	7
Figure 4.	Phi-scale showing the particle size distribution on the LANL 2016 round robin study. The average particle size was found to be 12.2 µm after analyzing over 3,000 individual particles. Note that when using the phi-scale, larger particles are numerically lower on the phi-scale and plot on the left side of the graph and vice versa for smaller particles	8
Figure 5.	(a) SEM image using the same 3.3 ratio of particle weight (mg) to IPA volume (ml) from the SDS study. (b) SEM image of SRM 1984 using a 35.0 to 1 ratio of particle weight (mg) to IPA volume (ml) from the SDS study.	9
Figure 6.	Phi-scale showing the particle size distribution from the current wet dispersion method on the NIST 1984 SRM. The average particle size was found to be 6.1 µm after analyzing ~3,000 individual particles	10
Figure 7.	NIST 1984 SRM sampled using wet dispersion technique with solvent composed of 100% LST.	11
Figure 8.	SEM image of NIST 1984 SRM using LST-IPA solvent and IPA post sampling wash	12
Figure 9.	Histogram of NIST 1984 particle size across five SEM stubs using two batches and three analysts.	13
Figure 10.	Histograms showing the variation in average particle size and distribution between different stubs and batches for one analyst	14
Figure 11.	Histograms showing the variation in average particle size and distribution between different analysts for two different stubs from one batch.	15
Figure 12.	(a) Histogram showing a normal distribution of 3,000 NIST 1984 particles analyzed using the LST wet dispersion method with a mean particle size of 15.0 μm. (b-c) Histograms showing distribution of randomly selected 300 particles from initial 3,000 particle set. Each sub-sample still has a normal distribution and a mean particle size of 15 μm.	16
Figure 13.	Histogram of the CeO ₂ particle size distribution after analysis of 333 particles using MAMA on SEM images collected from tubes using the LST heavy liquid wet deposition method	17
Figure 14.	Outlines collected from the DIA on NIST 1984 SRM showing large and small particle sizes. Work is still underway to train on the software and display particles with scale bars. There is some concern about the resolution of the smaller particles; it's unclear if this is instrument-limited or display-limited at this time.	18

Contents

Figure 15.	Four charts of particle size distribution generated by the Sympatec software for the CeO ₂ powders using various stirring speeds from 200 to 2,000 rpm. It appears values between 400 and 1,000 rpm give consistent average particle size values and expected bell shape distributions	19
Figure 16.	Optimal DIA pump speed (250) and stirrer speed (800) as determined by the shape of the distribution curve and the exact match to the average particle size listed (16.5 μ m) in the NIST 1984 SRM reference documentation.	20
Figure 17.	AFM topography, deflection, and phase imaging showing heavy recession of the NIST 1984 SRM into the carbon tape	21
Tables		
Table 1.	Test Matrix for DIA using NIST 1984 SRM	20
Table 2.	AFM NIST 1984 particle recession into carbon sticky tape analysis	22

Contents

1.0 Introduction

The primary goal of the scanning electron microscopy (SEM) biases project was to determine if there was any systemic error in the sampling, imaging, or analysis of the PuO₂ analyzed during the statistical design study (SDS), and if so, to develop a weighting algorithm for the current data.[1] A secondary goal was to determine the source of the error and, if possible, improve the sampling methodology for SEM analysis to reduce the need for future correction factors. A final goal was to mentor junior staff and help them develop expertise in morphological analysis of actinide particles.

Several important tools were used to achieve the goals of this project. The first was a National Institute of Standards and Technology (NIST) standard reference material for particle size distribution (NIST SRM 1984). These particles were run through the same wet dispersion sampling, SEM imaging, and particle morphology analysis methods used in the PuO₂ SDS to determine if there was intrinsic bias in the original data set. Although not a perfect morphological match, the NIST SRM 1984 powders are composed of some heavier elements, including tungsten (19.25 g/cm³), which should lead to similar particle behavior as the PuO₂ (11.5 g/cm³) powders used in the SDS. This approach was combined with the use of a new dynamic image analyzer (DIA) particle size analysis (PSA) instrument to measure the NIST standard to provide a comparative data set. The DIA provides a rapid particle image acquisition and analysis capability for bulk powder morphological statistics.

1.1 Statistical Design Study

The SDS was a Pacific Northwest National Laboratory (PNNL) project funded by the Department of Homeland Security's National Technical Nuclear Forensics Center to determine nuclear forensics signatures of plutonium oxide (PuO₂) specimens based on varying select processing conditions. As such, a bench-scale PuO₂ processing capability previously established at PNNL was used to produce 76 separate batches of roughly 10.0 g Pu per batch. This set of experiments varied six different processing conditions, including Pu concentration (10, 30, 50 g Pu/L), nitric acid (HNO₃) concentration (1, 2, or 3M), temperature (30 or 50 °C), addition/digestion times (0, 20, 40 min), strike conditions (direct or reverse), and physical form of the oxalic acid (solid or solution).

The feed material used in this study was PuO_2 . The as-received oxide was dissolved in nitric acid with some fluoride added to accelerate dissolution. Impurities were removed from the resulting solution via anion exchange. Then, the Pu was precipitated as plutonium (III) oxalate, $Pu_2(C_2O_4)_3\cdot 10H_2O$ [2]. After conversion to PuO_2 by calcination, each sample was coned and quartered to isolate multiple aliquots. One of these aliquots was subject to morphological characterization using SEM and the Morphological Analysis for Material Attribution (MAMA) software.¹

1.2 Morphological Particle Analysis

It is generally assumed that various processing parameters involved in actinide material production, including chemical composition of the feed material, precipitation, and calcination conditions, can affect the morphology of the resulting powders. These parameters include particle size, shape, and density [3]. Understanding the effects of such parameters may help

Introduction 1

¹ https://searchworks.stanford.edu/view/12022584

reveal the production history of intercepted nuclear material. However, only a few systematic studies have been performed to investigate the morphological characteristics of nuclear material production, with most focusing on easier-to-handle uranium compounds [4-6]. The successful acquisition of useful and representative data from powder samples is ultimately dependent on the method used to sample the powders for imaging. It is critical that this technique produces an accurate representation of the bulk powders that is free of biases. Actinide particle analysis (particularly in transuranic materials) is further complicated by the need for a method that is radiologically safe and has a low risk of contaminating the laboratory where powders are prepared, and the instrumentation used to analyze them.

Introduction 2

2.0 Experimental Methods

Successful acquisition of representative morphological data from actinide powder samples is highly dependent on the sampling method used for imaging. Criteria for successful mounting also include radiological safety constraints. Therefore, one must achieve sufficient loading for particle statistics while keeping the activity within the bounds of benchtop limits (1.68 μ Curie (Ci)). Additional radiological constraints include sufficient adhesion of particles to the substrate to mitigate contamination risks. All these constraints must be met while maintaining a representative sample from the bulk powder.

2.1 Dry Particle Sampling

Previously, dry sampling involved the dispersion of dry PuO₂ powder onto an SEM stub covered in carbon tape. Statistically, this approach has proven adequate for delivering a representative sample, but it is limited in dispersion control and the resulting activity of the mount surface can be difficult to control. The extent of the dispersion control is analyzed in Section 3.1. Contamination risks are still present, as tap tests within radiological fume hoods have been observed to remove PuO₂ powder from the carbon tape.

2.2 Wet Particle Sampling

Wet sampling was chosen as the primary means for particle deposition in this study due to its improved control of the loaded activity, tailorable dispersion based on loading and suspension media, and improved retention of the sample. The improved retention of the PuO₂ was discovered somewhat accidently as the isopropyl alcohol (IPA) used for final deposition on the carbon tape slightly dissolved the glue, resulting in more particles sinking into the substrate than would occur with dry dispersion. This was confirmed by atomic force microscopy (AFM) analysis on a SEM stub (Section 5.0). The result is an SEM stub in which the particles are held more securely than in dry dispersion. Subsequent tap tests of over 100 wet dispersion mounts have resulted in zero detectable particles being dislodged. Compared to dry dispersion sampling, spacing of particles on the SEM substrate is highly tailorable based on the liquid-to-particle ratio.

The development of this process began during the SDS, in which the powder, suspension media, loading, and mounting substrate were all varied. The results of that testing and optimization study gave the following procedure, which was ultimately used to sample all the particles for the 76 runs used in the SDS study.

Nominally, 10 mg of PuO₂ powder was measured out and dispersed in 3 mL of IPA within a high-contamination area (HCA) glove box. For NIST 1984 powders prepped on a bench top, the ratio of powder to IPA was adjusted to 35 mg SRM to 1 mL of IPA. These suspensions were homogenized by mixing for 60 seconds at 2,000 rpm on a vortex mixer. Immediately after mixing, a 5-µL droplet of the suspension was transferred by pipette to the center of a 25.4-mm aluminum (AI) planchette covered with carbon tape. After the IPA had visibly dried (i.e., evaporated), the planchette was inverted and vigorously tap tested within the glove box to ensure any loosely mounted particles were removed. The sample was then transferred to the center of an AI pan (51 mm inside diameter x 10 mm depth) within the antechamber. This AI pan was used both as a secondary containment barrier for loose or flighty particles and to cleanly transfer the AI planchette to a surface that had never encountered the HCA environment for

Experimental Methods 3

safe handling and transfer to the SEM. A secondary tap test was performed in a fume hood before the sample was sealed and transferred to the SEM. The loading was selected such that the activity of each sample was between 1-2 million milli Roentgen equivalent man (rem) dose per minute (dpm) alpha (α) radiation.

Unfortunately, this method led to a heavy bias toward smaller/lighter particles due to Stokes' law-based settling of heavy PuO₂ out of suspension within the IPA. The statistical analysis of this can be found in Section 3.2. A large portion of this study involved the development of a second iteration of wet dispersion that would retain the benefits of the wet sampling method (i.e., activity loading control and contamination mitigation) while removing the morphological biases introduced by this first iteration described here.

2.3 Heavy Liquid Particle Sampling

A second wet dispersion technique was introduced to improve the capture of larger particles. The hypothesis, bases on Stokes' law calculations, was that a heavy liquid with higher density and viscosity could hold the larger PuO₂ particles in suspension nearly six times as long. Ultimately, lithium heteropolytungstate (LST) was chosen for its non-toxic behavior and because its density and viscosity are nearly four times those of IPA.

Figure 1 compares the settling rates of 700 mg of the NIST 1984 SRM mixed in 20 mL of IPA and LST, respectively. It's clear in Figure 1b that a large portion of the NIST 1984 SRM has already started to settle on the bottom of the vial. This is in stark contrast to the particles in suspension in the LST mixture, in which no discernable color variation could be observed after 60 seconds. In fact, no discernable settling via a color variation was observed in the LST mixture after several days of settling.

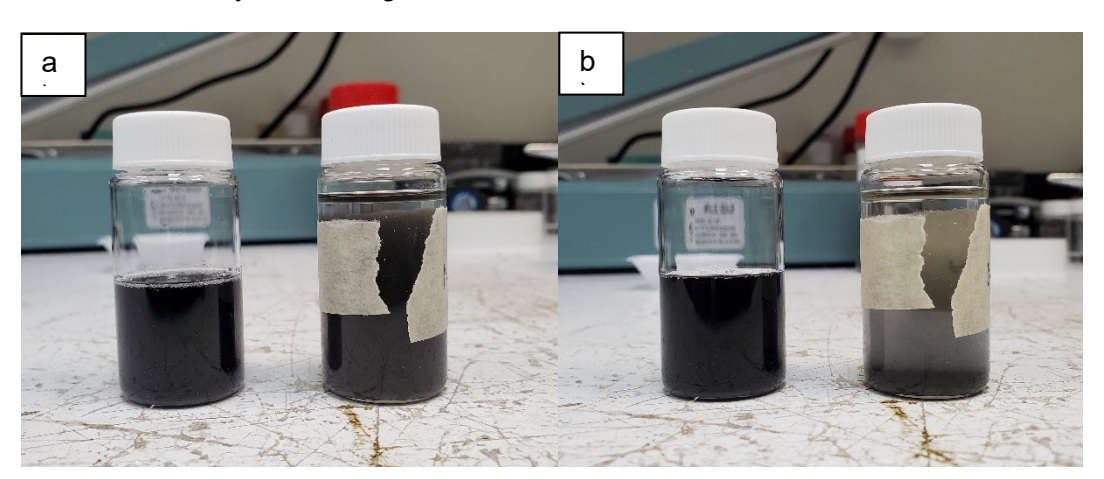


Figure 1. Images comparing the settling behavior of the heavy liquid (left) and the IPA (right) after (a) 10 sec and (b) 60 sec from removal of the vortex mixer. It's clear the heavy liquid (LST) has a much slower settling rate than the IPA.

These suspensions were homogenized by mixing for 60 seconds at 2,000 rpm on a vortex mixer. Unfortunately, the LST crystallized out of solution when deposited on the SEM stub with carbon sticky tape. Therefore, LST can be used as the suspension media in which the representative particle aliquot is procured, but it cannot be used as the medium in which the particles are dispersed on the SEM substrate. Figure 7 shows an SEM image in which LST crystals have completely covered the sample. A detailed analysis of the development of a

Experimental Methods 4

washing method to remove the LST after the representative aliquot has been sampled can be found in Section 3.3.

2.4 **SEM**

Samples were imaged using three SEMs: FEI Quattro ESEM, FEI Quanta 250 field emission gun (FEG)-SEM, and JEOL 7001F SEM. Samples were imaged using both secondary electron (SE) and backscattered electron (BSE) detectors. The samples were imaged at high resolution (2,048 x 1,887) at various magnifications from 500x to 2,500x. Samples were collected in a raster pattern that progressed from the top left of the sample to the bottom right and ensured no particles were imaged twice. Both analyst-captured images and automated mapping image acquisition were used.

2.5 MAMA

Two components of a population of particles were studied here. First, particle size distributions were characterized by outlines of particles created in the MAMA software, developed by Los Alamos National Laboratory (LANL). Particle morphology in this study was predominantly focused on the shape of the individual particles of a given processing or powder batch based on their outlines. These features were analyzed using version 2.1 of MAMA. A minimum of 2,000 particles was desired from each powder batch to determine particle morphology statistics. Analyzed metrics, including pixel area, minimum and maximum diameter, circularity, and ellipse aspect ratio, were quantified for each particle.

There is a question in the nuclear forensics community as to what defines a particle. For this study, we define a particle as a singular entity that has no contact with other materials at its edges, has distinct internal textural features that reasonably allow it to be differentiated from other particles, and shares SE and BSE characteristics with the sample as a whole. We did not analyze particles that were smaller than approximately 2 microns (μ m), as it is ambiguous whether this represents a true particle created by processing or it is a piece of material broken off from a larger particle.

2.6 Dynamic Image Analysis

The DIA method was implemented with a Sympatec QICPIC. This instrument performs high-speed image analysis using a pulsed light source. Illumination times are in the range of nanoseconds and particle outlines are optically captured with a high-resolution, high-speed camera at up to 500 frames per second. The QICPIC software performs similar morphological analysis to that of the MAMA software, and reports metrics such as pixel area, circularity, and ellipse aspect ratio for each particle.

Experimental Methods 5

3.0 SEM & MAMA

3.1 Dry Sampling

3.1.1 NIST 1984

The primary goal of this effort was to generate a statistically robust (i.e., 3,000+ particles) analysis of the dry dispersion sampling method for SEM imaging. This analysis used NIST 1984 SRM images from a previous round robin study conducted by LANL in 2016.[7, 8] Figure 2 shows a sample SEM image used in this effort. The secondary goal of this effort was to train staff members who were new to the project on how to capture particle morphology statistics using MAMA software. Several areas of concern with previous dispersion methods can be seen in Figure 2, including areas of clumping and overlap in which exact particle boundaries are unknown.

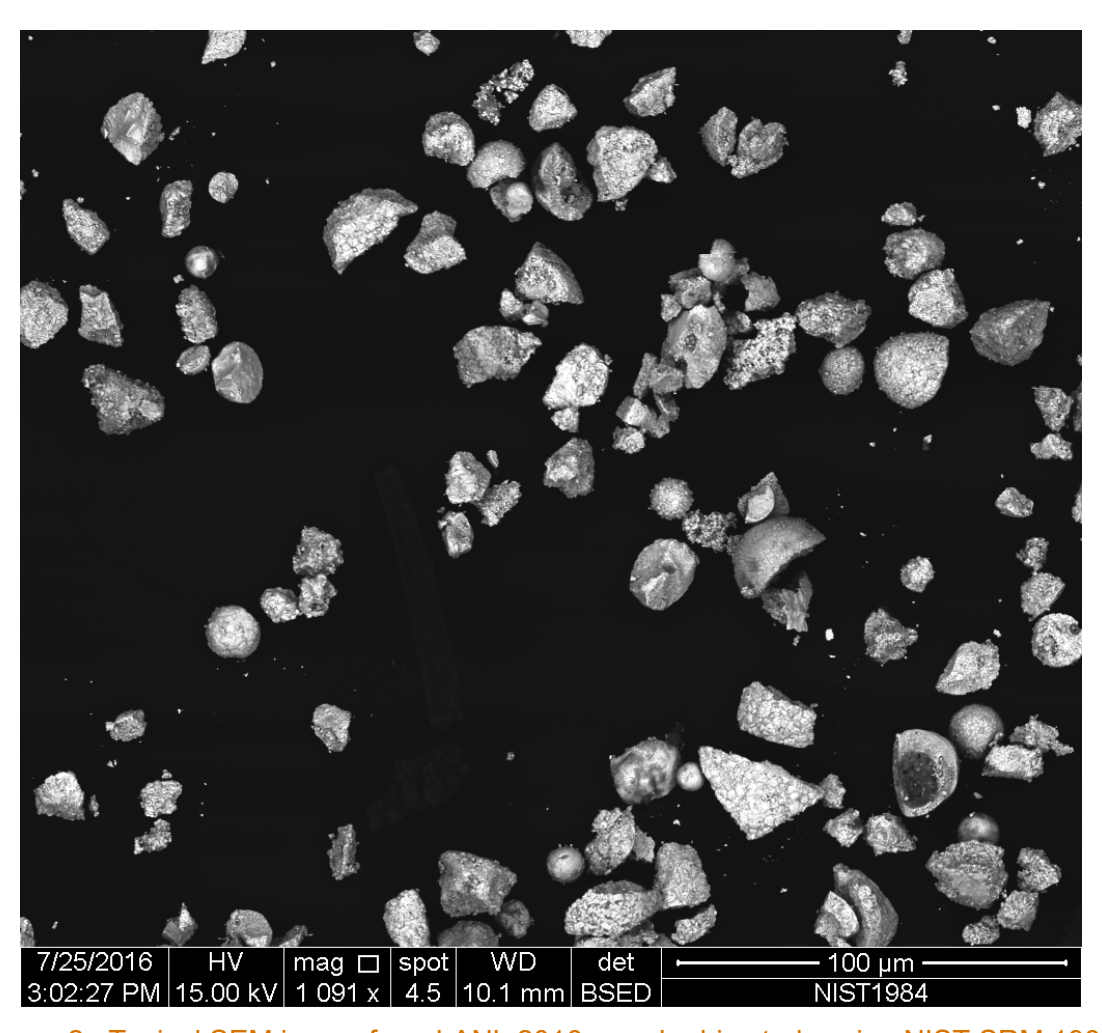


Figure 2. Typical SEM image from LANL 2016 round robin study using NIST SRM 1984.

Ultimately, over 3,000 particles were analyzed and compared to the certified particle distribution of the NIST 1984 particle. The method involves segmenting particles from an SEM image based on grayscale. The resulting particle areas are fitted with major and minor ellipses, which are then converted to a prolate ellipsoid. The reported particle size is the average diameter of the

three resulting axes. Figure 3 provides a histogram of the data, showing the average particle size as 12.22 μ m. This is ~30% smaller than the certified average particle size of 17.1 μ m, indicating a biasing toward smaller particle sizes from the dry dispersion method. The major difference between the LANL study and the NIST certification is that NIST separated the particles by sieve into four size groups before SEM analysis. It is unknown at this time exactly why the removal of the sieving step would bias toward smaller particles, but it appears to be the only major difference in analysis.

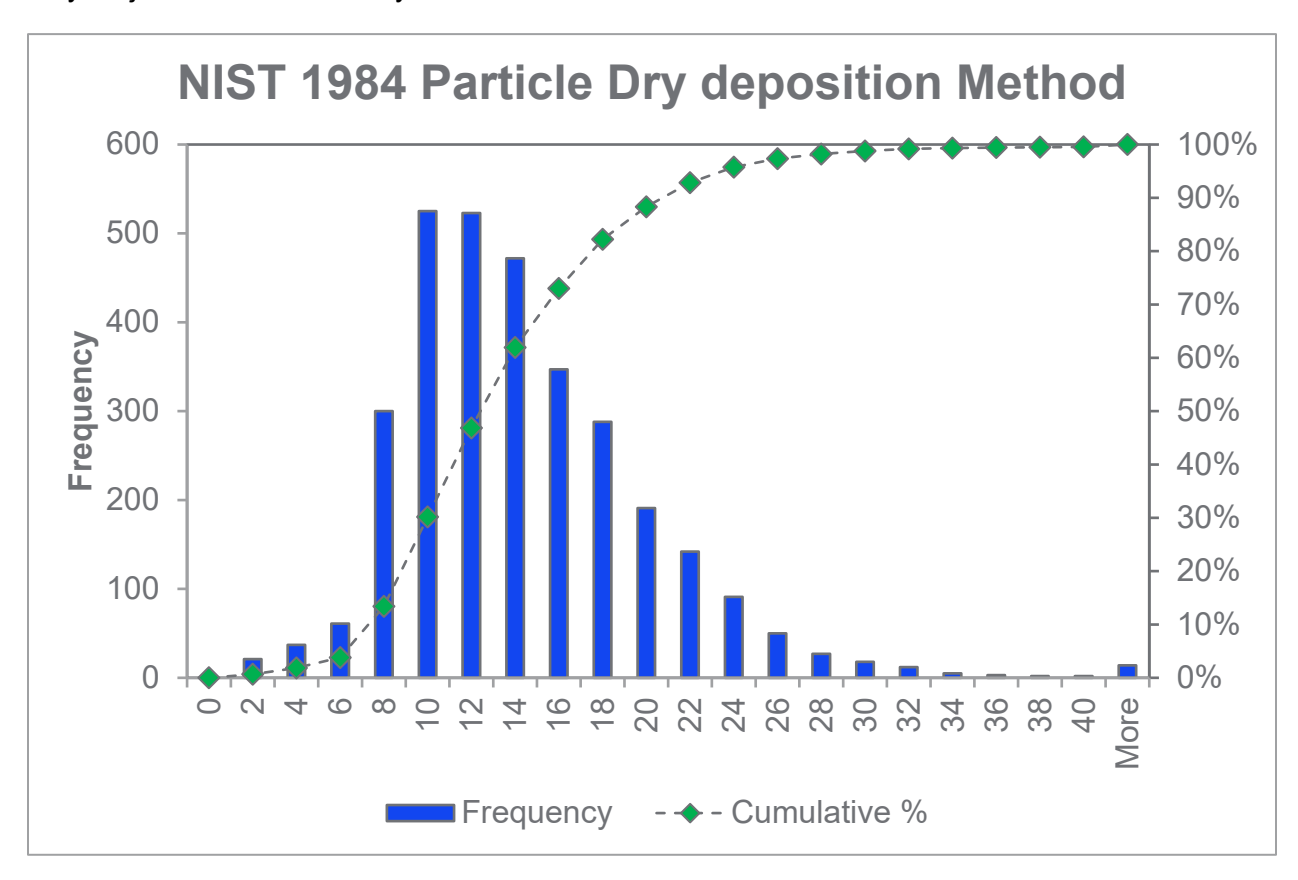


Figure 3. Histogram showing the particle size distribution found within the images captured for the LANL 2016 round robin study. The average particle size was found to be 12.22 µm after analyzing over 3,000 individual particles.

Assuming near equilibrium conditions, particle size distributions of materials formed by precipitation from a solution are almost always log-normal. Thus, if visualized in linear space, non-normal distributions (i.e., bimodal distributions) often result. This makes traditional statistical analysis and comparison of two populations a non-trivial exercise. In the geological sciences, the phi-scale is used, where $\text{phi}(\phi) = -\log_2(S)$, S is the grain size in millimeters. The phi-scale is advantageous because it gives equal significance to changing size ratios and allows for the comparison of a large range in particle sizes, all while retaining resolution at the smaller particle sizes. As a result, it will help determine if a given sample's particle size distribution was biased by the sampling method or by the process used to create the particles. Figure 4 shows a plot of the ~3,000 dry dispersion particles using the phi-scale method. Note the nice bell curve shape, indicating a normal distribution with little evidence of a bimodal separation.

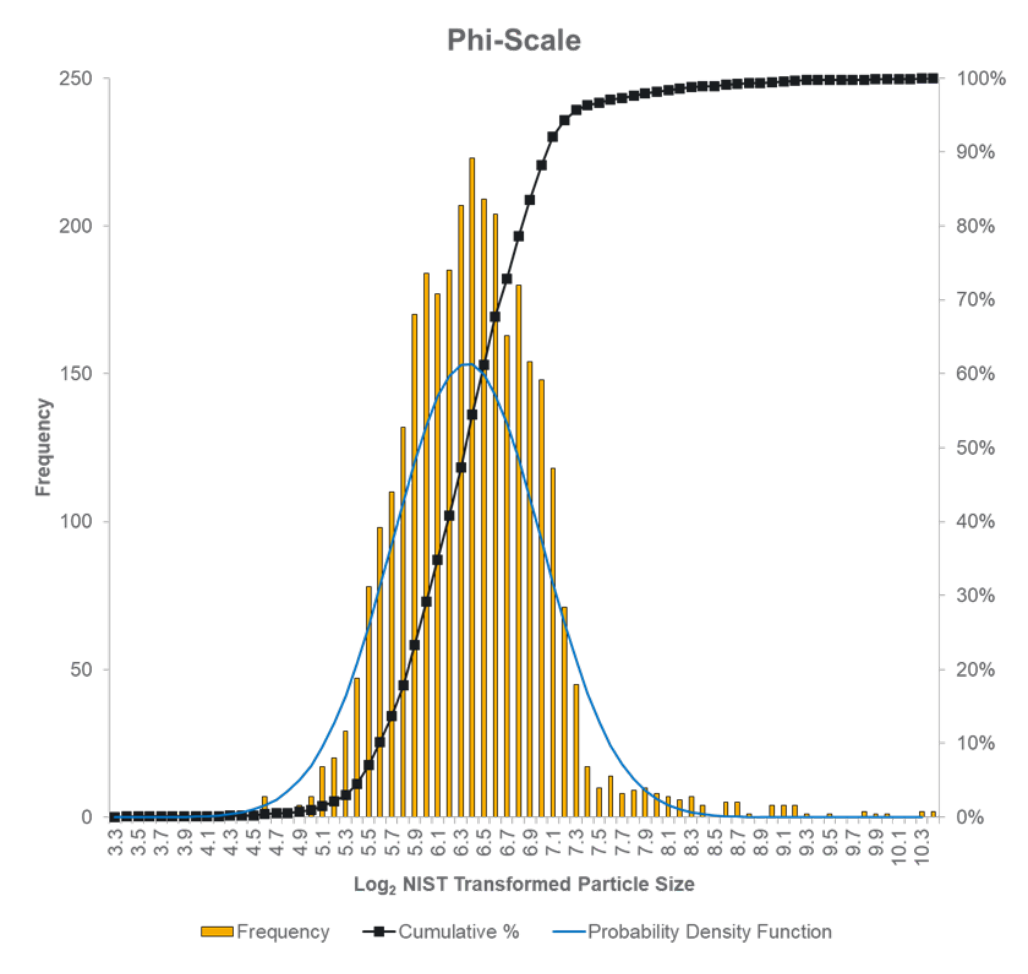


Figure 4. Phi-scale showing the particle size distribution on the LANL 2016 round robin study. The average particle size was found to be 12.2 µm after analyzing over 3,000 individual particles. Note that when using the phi-scale, larger particles are numerically lower on the phi-scale and plot on the left side of the graph and vice versa for smaller particles.

3.2 Wet Sampling

3.2.1 NIST 1984

Wet dispersion sampling, as performed in the SDS, was conducted. The only modification was to the loading ratio for the NIST 1984 standard. It was found that using the same ratio (3.3 to 1) of weighed particles (mg) to volume of IPA (mL) resulted in a sampling density that was too disperse, as shown in Figure 5a. Two more SEM stubs were prepared in which the loading ratio was increased by 5 and 10 times, respectively. It was found that 10x loading resulted in an acceptable particle density, as can be seen in Figure 5b. Comparing Figure 1 to Figure 5b, we can see that there is an improvement in particle spacing with less particle overlap and touching. This is one advantage of the wet dispersion method: the ability to tailor the loading such that the MAMA user has fewer interpretations to make regarding overlapping or touching particle boundaries. A second and equally important benefit when working with high-activity radionuclides is the ability to precisely deposit a specified activity of radioactive material on each SEM stub.

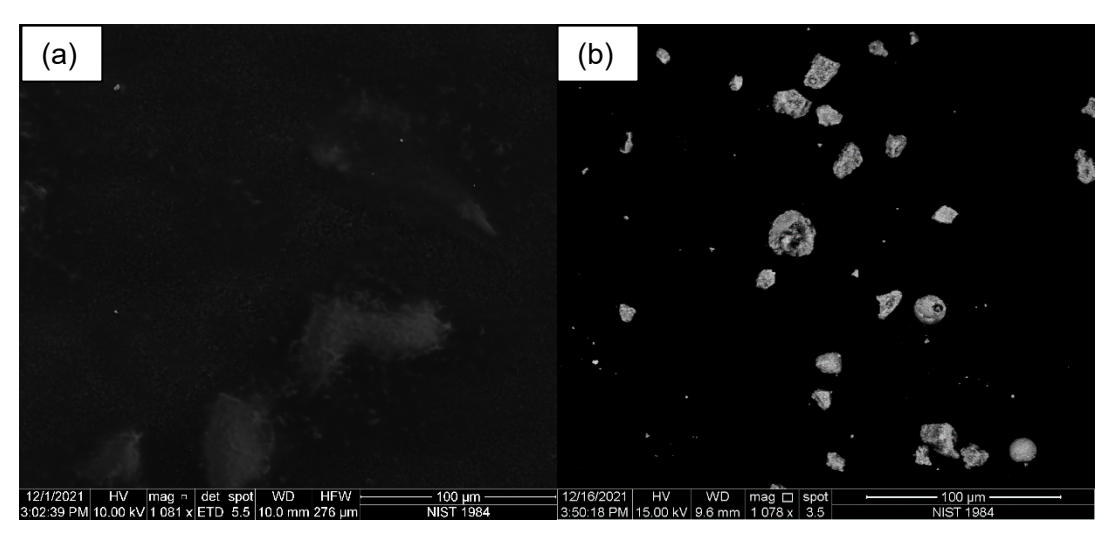


Figure 5. (a) SEM image using the same 3.3 ratio of particle weight (mg) to IPA volume (mL) from the SDS study. (b) SEM image of SRM 1984 using a 35.0 to 1 ratio of particle weight (mg) to IPA volume (mL) from the SDS study.

Using a 35.0 to 1 ratio, over 3,000 particles were analyzed using MAMA from ~100 images. An average particle size of 6.1 μ m was calculated, which is ~65% smaller than the certified value for the NIST 1984 SRM. This indicates a dramatic bias toward smaller particles from the first iteration of the wet dispersion method as implemented in the SDS. This indicates that the original method used in the SDS study does not accurately capture a representative sample from the population. This is likely due to larger, heavier particles settling at a rate faster than what can be sampled by pipette extraction. Using the phi-scale transformation, an additional trend was found in the data. A large bimodal distribution focused on the smaller grain sizes of 2.4 and 9.6 μ m. The exact cause of this distribution is currently uncertain, but investigations are underway.

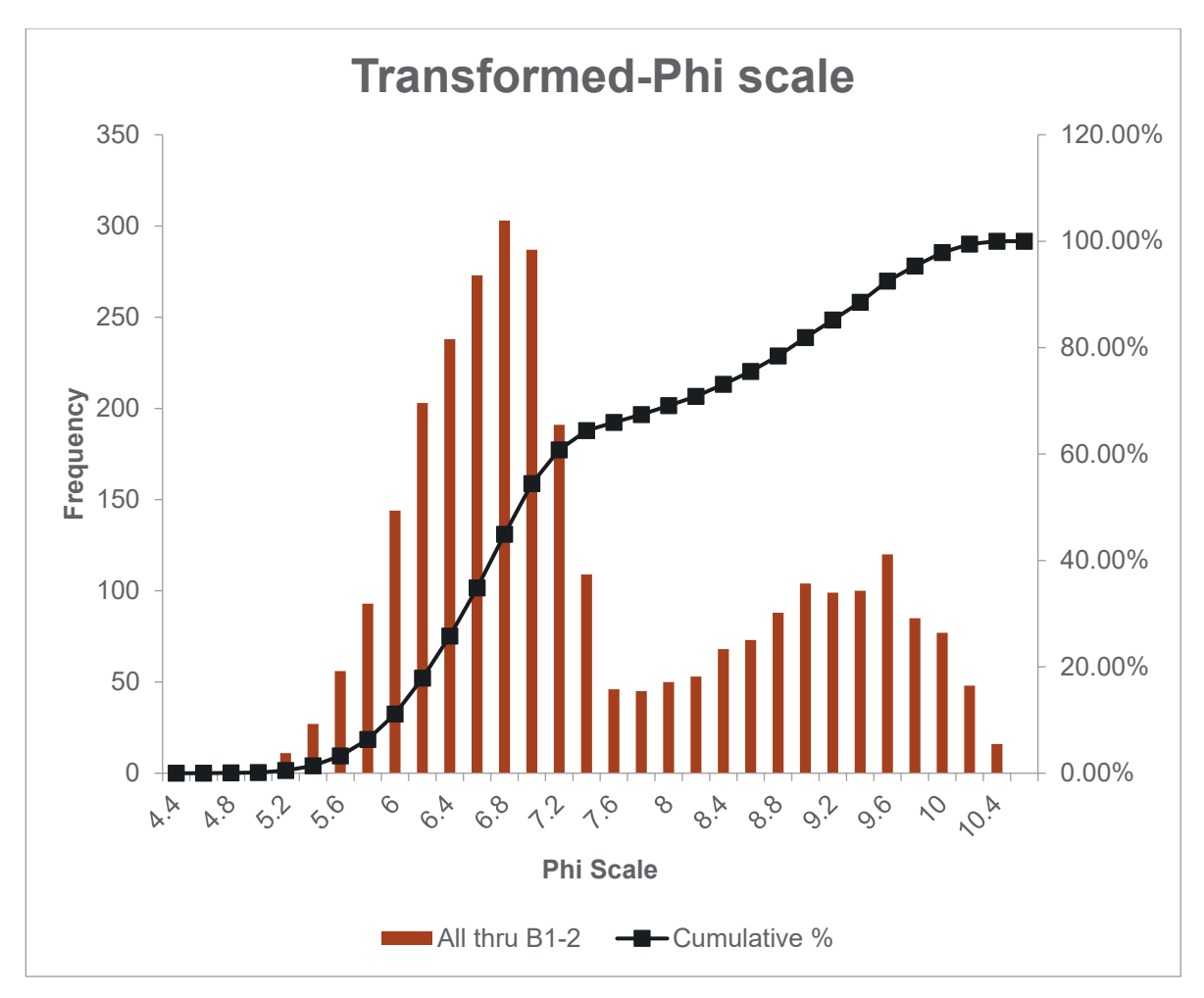


Figure 6. Phi-scale showing the particle size distribution from the current wet dispersion method on the NIST 1984 SRM. The average particle size was found to be 6.1 μm after analyzing ~3,000 individual particles.

3.3 Heavy Liquid Wet Sampling

3.3.1 NIST 1984

Initial work involved replacing IPA entirely with the LST solution. This resulted in heavy crystallization of the lithium tungstate from the LST solution as the water evaporated. Figure 7 shows an SEM image in which no NIST SRM 1984 can be seen as the entire sampling droplet has crystalized.

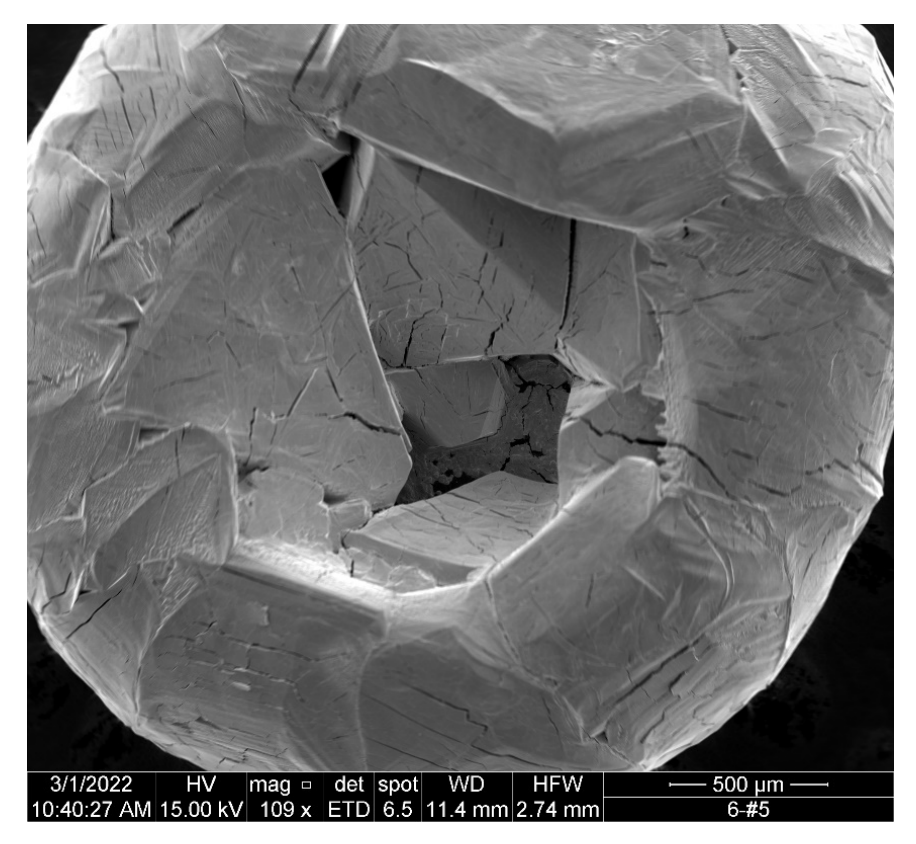


Figure 7. NIST 1984 SRM sampled using wet dispersion technique with solvent composed of 100% LST.

As a result, a washing method was introduced that removed the LST from the particles. LST is soluble in IPA and was therefore used to thin the particle/LST mixture. After the 5 μ L aliquot was taken from the main 35.0:1 particle mixture (see above), it was directly pipetted into a separate scintillation vial. Five mL of IPA was then added to this vial. Using a steady swirling motion, the particles were simultaneously washed of the LST and were concentrated into a pile at the bottom of the vial. This pile was then extracted by a pipette and deposited directly onto the SEM stub. It's important to note that no bias was introduced in the washing step because we were only washing the particles extracted by the 5 μ L aliquot and it was easy to see the pile of particles at the bottom of the vial after swirling. After the propanol had visibly dried (i.e., evaporated), the planchette was ready for imaging. The results of this process can be seen in Figure 8.

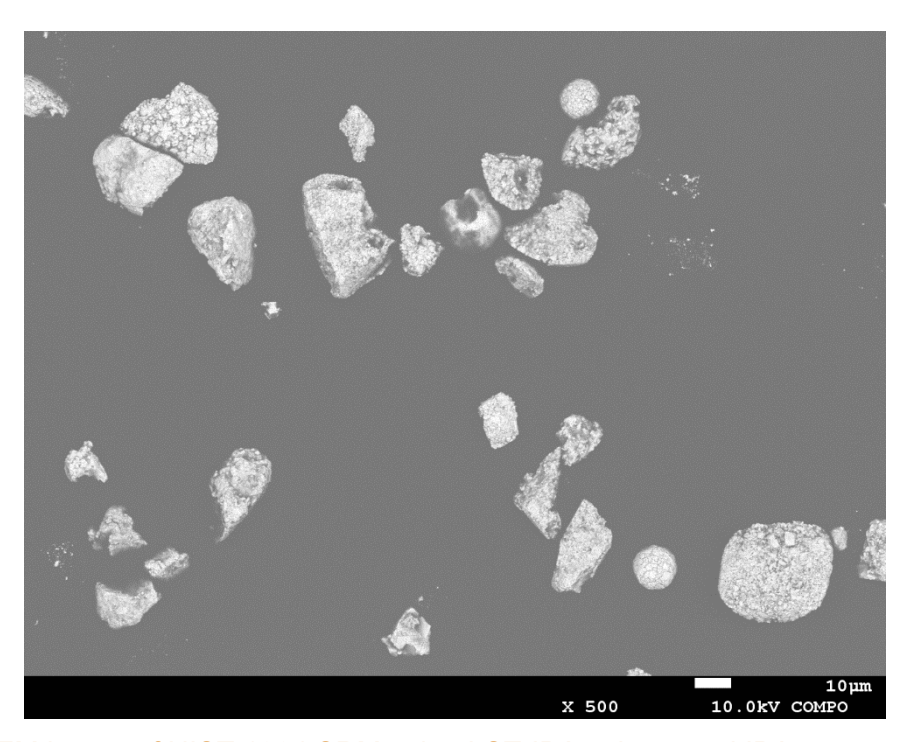


Figure 8. SEM image of NIST 1984 SRM using LST-IPA solvent and IPA post sampling wash.

Due to the success of the improved wet dispersion technique, statistical analysis was performed to determine the average particle size and distribution obtained via SEM analysis and MAMA. Two additional PhD interns were recruited for this effort. Three analysts measured a total of 3,689 particles across five SEM sample stubs and determined that the average particle size was 12.7 µm.

The phi-scale histogram of the data can be found in Figure 9. This data is ~25% lower than the certified value of 17.1 μ m and outside of the \pm 2.2 μ m uncertainty reported. This is significantly better than the average grain size (6.1 μ m) reported by simply using wet dispersion with IPA and similar to the dry dispersion method value of 12.2 μ m. The shape of the distribution is also improved (i.e., more normal), suggesting that this method captures a more representative sample than the dry dispersion technique. Perhaps most importantly, this improved technique is very consistent in the amount deposited on the SEM stub, which from a radiological safety standpoint is very advantageous.

It is believed that the remaining 25% discrepancy between the LST wet dispersion method and the sieving and dry dispersion method used in the NIST certificate is due to particle recession into the carbon tape. This is investigated in Section 5.0 using AFM and a primitive correction factor is introduced.

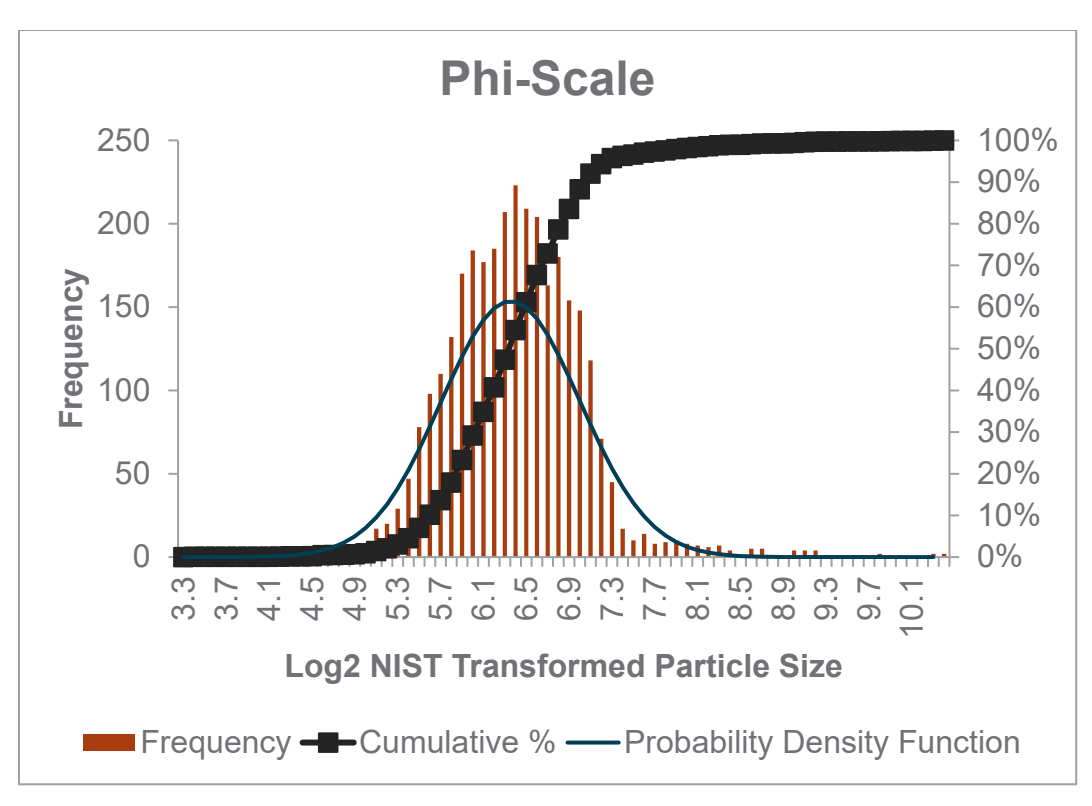


Figure 9. Histogram of NIST 1984 particle size across five SEM stubs using two batches and three analysts.

To test the reproducibility of the new method, we compared the results of two different aliquots from the same sample deposited onto two different SEM stubs. Figure 10 is a histogram from individual stubs using two NIST 1984 SRM-LST batches from the same lot of powder. Overall, the bimodal distribution that was so prevalent in the pure IPA wet dispersion method is suppressed when using LST. Second, the major modes have means that are significantly higher than the reported average, somewhere in the 12.2-15 μ m region. It can clearly be seen that the first batch (B1HL A and B) has means that are closer to the 14-15 μ m mark while the second batch (B2HL 1 and 2) has means closer to the 11-12 μ m mark. At this point, the reason for the discrepancy between the two batches is still unknown, but it is a good reminder that the overall precision and accuracy of the SEM method are heavily reliant on accurate and consistent sampling.

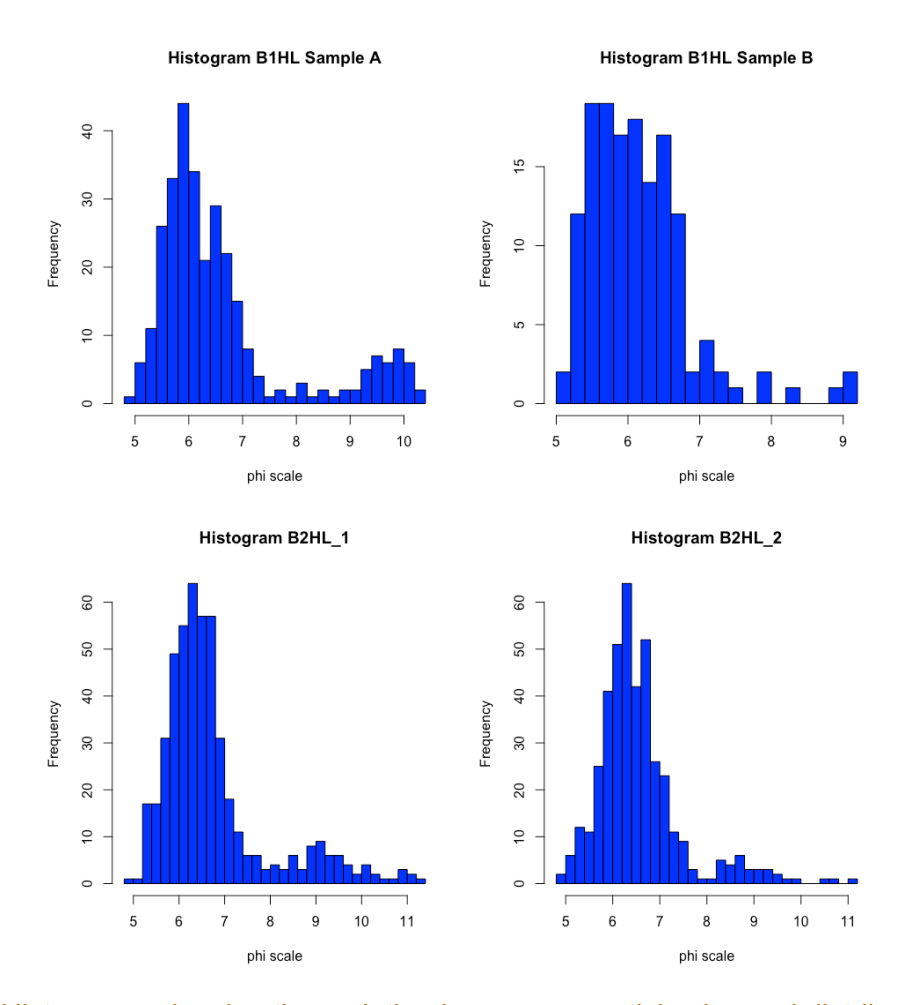


Figure 10. Histograms showing the variation in average particle size and distribution between different stubs and batches for one analyst.

Statistical analysis was performed to determine if there was significant difference between data sets from the three analysts. Figure 11 shows the histogram data for two SEM stubs from the first batch for the three analysts. Statistically different data were determined through p-value analysis with a null hypothesis that there was no significant statistical variation. The results indicate that the average particle size and distribution has a statistically significant dependence on the analyst. Using just the first stub from the first batch (B1HL-A), it was determined there was a p-value of 0.416 between analysts 2 and 3 but a p-value of 1.366E-6 and 5.299E-6 between analysts 2 and 3 in comparison to analyst 1, respectively.

It's important to note that in an attempt to alleviate initial bias, no limitations were given to the analysts prior to beginning their analysis, (e.g., no definitions or boundaries were set for their interpretation of what is, and what is not, a particle). The statistically significant difference in the subsequent results perhaps is not surprising, but it nevertheless strengthens the argument that as a community, certain initial conditions (e.g., lower limit on segmented particle size, are we or are we not going to include overlapping particles) must be agreed upon to produce meaningful results and comparisons. Another potential way to alleviate this would be to incorporate automated computer segmentation, eliminating any potential bias introduced by the MAMA analyst.

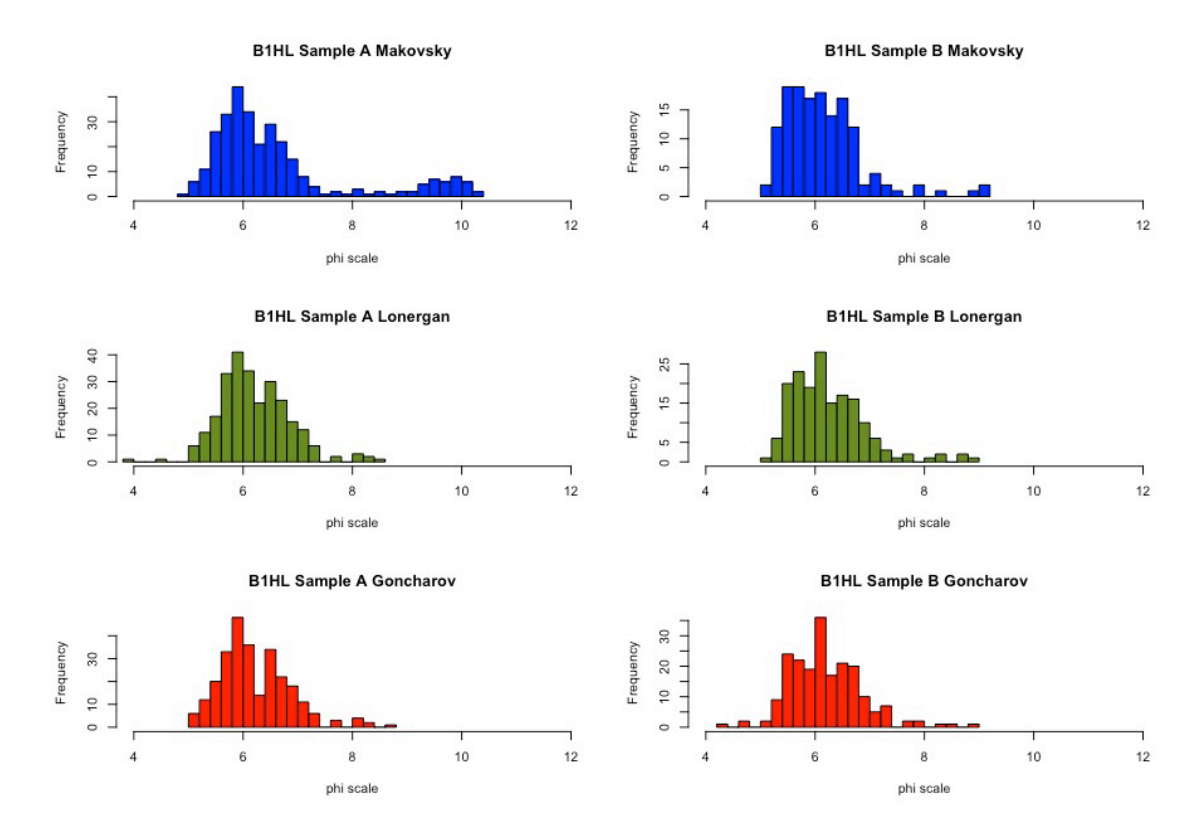


Figure 11. Histograms showing the variation in average particle size and distribution between different analysts for two different stubs from one batch.

One major limitation to the coupled SEM/MAMA technique is the significant time it takes for particle segmentation. Initially, it was believed that several thousand particles from each sample were needed to establish statistics representative of the population. However, as we've shown in this study, this was likely due to poor sampling techniques, which ultimately led to erroneous conclusions about the efficacy of the method.

We have shown that with the old method there is a significant bias toward smaller grain sizes and the resulting particle size distributions are quite poor. With the introduction of LST as the sampling media and usage of visualizing data in log-space, we have eliminated the bimodal nature of the resulting particle size distributions and improved the accuracy of the average particle size. However, the question still remains as to how many particles are needed to capture a representative sample.

To address this, a statistical experiment was performed. Note, this is only meaningful for populations and samples with normal distributions, which we've now shown we can produce. In this experiment, 3,000 random numbers were generated, having a normal distribution and a mean of 15 and standard deviation of 5. From the 3,000 randomly generated numbers, three samples were taken, each consisting of 300 randomly selected values from the population of 3,000. The mean, variance, and standard deviation were determined from the three samples, and using simple statistical hypothesis testing, we evaluated the samples to determine if they were statistically indistinguishable from the population.

The results in Figure 12 show that the three sub-samples are indeed statistically indistinguishable from the population. Extrapolating this to our sampling strategy, we can be

confident that we may only need to segment and analyze hundreds of particles and not thousands, saving many hours of MAMA analysis and labor costs for future projects.

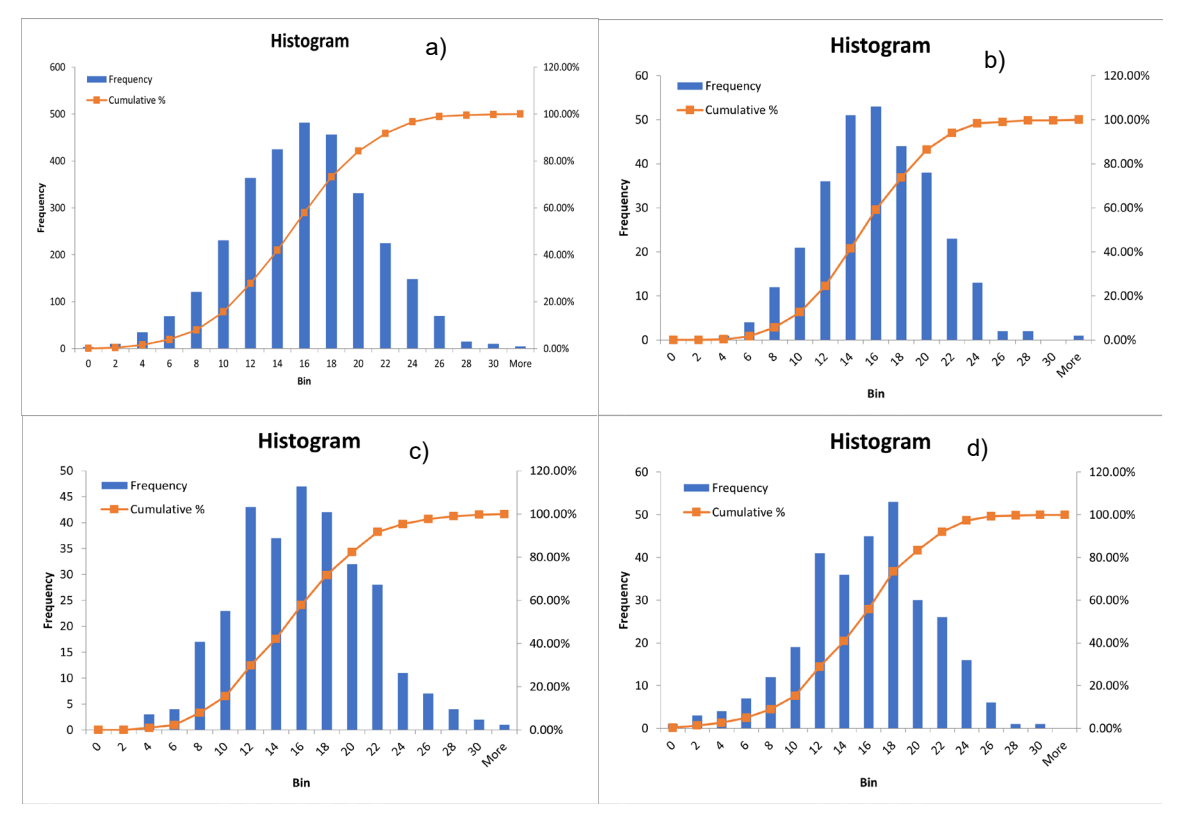


Figure 12. (a) Histogram showing a normal distribution of 3,000 NIST 1984 particles analyzed using the LST wet dispersion method with a mean particle size of 15.0 μ m. (b-c) Histograms showing distribution of randomly selected 300 particles from initial 3,000 particle set. Each sub-sample still has a normal distribution and a mean particle size of 15 μ m.

3.3.2 CeO₂

Given the success of the LST wet dispersion method in correcting the heavy biases toward smaller particles sizes and bimodal distribution found in the IPA wet dispersion method, a surrogate material was desired to ensure the heavy liquid wet sampling method would work well with actinide materials. In addition, procedures, equipment, and shielding that would be used for PuO₂ were implemented to ensure the transferability of the method and to train staff. A CeO₂ powder was chosen for its similar bonding structure and atomic mass, and because it would allow correlation to statistics generated by the PSA. Again, the goal was to show that the new LST deposition method removed the heavy bias toward small particles that was prevalent in the original IPA wet deposition method.

Two SEM stubs were prepared to ensure processing consistency. An average particle size of \sim 11.55 µm was calculated from analysis of 333 particles. This is in good agreement with the PSA data shown in Section 4.1. Interestingly, in the histogram (Figure 13), the highest frequency peaks are somewhat below the average around the 4 µm mark. A somewhat long tail extends past the initial peak into larger grain sizes but never really resolves into a clear bimodal distribution. Comparing this to the PSA data in Figure 15, a similar tail is shown. It should be

noted that there is still open debate about the exact number of particles needed to accurately determine particle size statistics. Although more is always better, the ability of the SEM/MAMA analysis to match the average grain size results of the PSA, using somewhere between 10,000-100,000 particles, with only 333 particles is a good sign that a representative aliquot may not require the thousands of particles often considered essential.

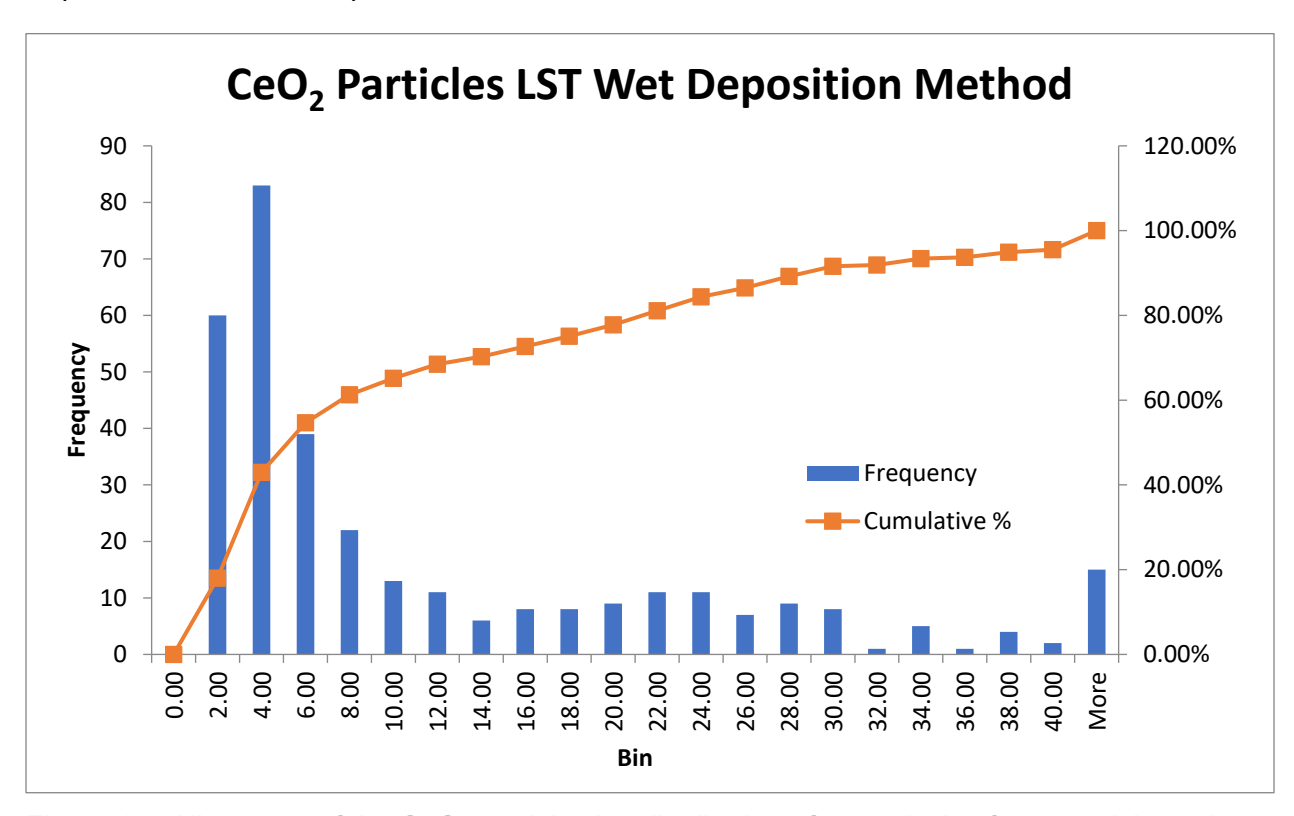


Figure 13. Histogram of the CeO₂ particle size distribution after analysis of 333 particles using MAMA on SEM images collected from tubes using the LST heavy liquid wet deposition method.

4.0 Particle Size Analyzer

4.1 Calibration

During the second quarter of fiscal year 2022, the Sympatec Inc. QICPIC DIA was installed and calibrated by a Sympatec representative, and initial training began on CeO₂ processed from the SDS. As mentioned in Section 2.6, the high-speed camera used in this technique is capable of 500 frames per second, allowing for millions of particles to be analyzed within a few hours. This capability has the potential to revolutionize the ability to perform accurate and statistically relevant PSA, easily reducing the time and effort needed to capture accurate and precise average particle size by orders of magnitude compared to the current SEM and MAMA analysis methods. Note that the DIA technique only captures a black and white image (Figure 14 shows several particles), limiting its ability to capture any relevant intra granular information. Therefore, all morphological features associated with the surface or texture of the particle will still require SEM or transmission electron microscopy analysis to capture.

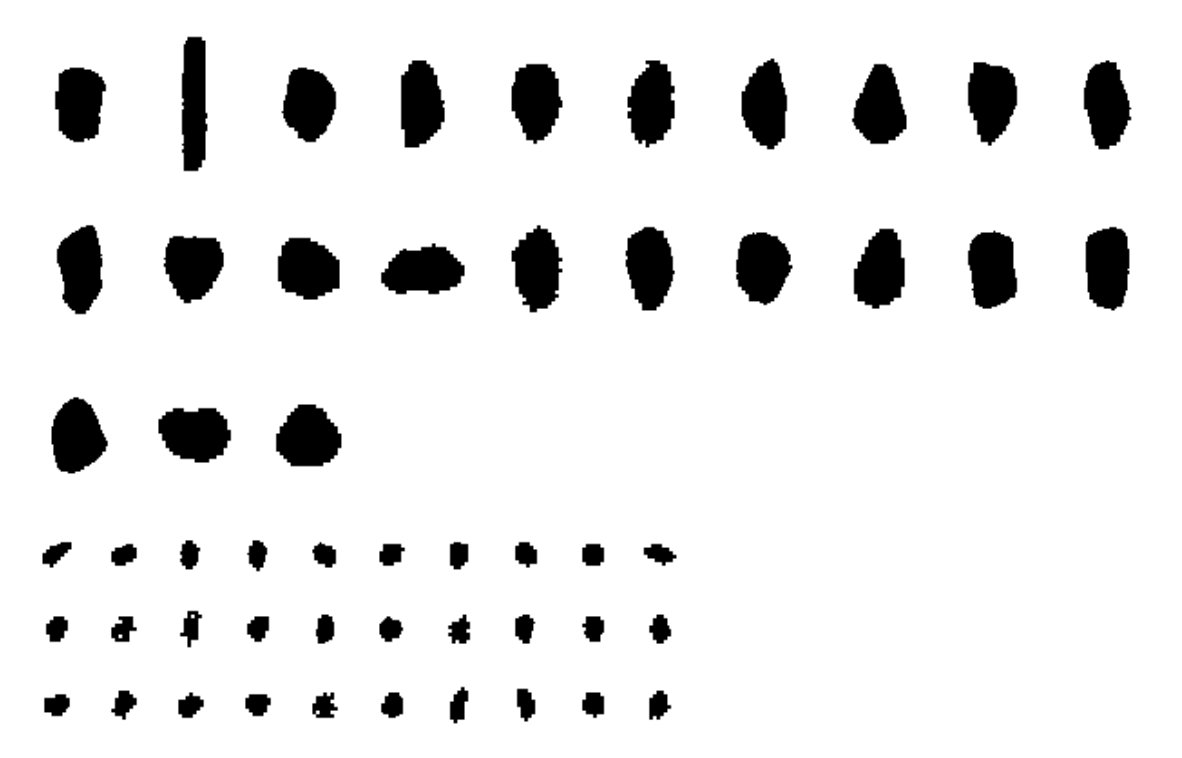


Figure 14. Outlines collected from the DIA on NIST 1984 SRM showing large and small particle sizes. Work is still underway to train on the software and display particles with scale bars. There is some concern about the resolution of the smaller particles; it's unclear if this is instrument-limited or display-limited.

Initial training on the DIA was performed with CeO_2 . Part of the initial calibration of the DIA is understanding the effects of particle loading, stirring speed, and pump speed. The DIA has an automatic loading feature that indicates when the particles have been correctly loaded. During initial training, powders were loaded until this function indicated proper loading. With the initial CeO_2 powder studies, pump speed was fixed at the recommended 100 revolutions per minute (rpm) value. With that said, a series of tests were performed in which the stirrer speed was varied. Figure 15 shows a series of four measurements run with CeO_2 in which the stirrer was

Particle Size Analyzer 18

ramped from 200 to 2,000 rpm. Although a certified particle size was not known for these materials, it seems that somewhere between 400 and 1,000 rpm is sufficient. An average particle size of 10.89 μ m was determined between these two stirrer speeds, and both plots show a regular bell shape distribution for the particles. Interestingly, it appears that a stirrer speed of 2,000 rpm was too fast creating large air bubbles that were analyzed as particles, nearly tripling the average particle size.

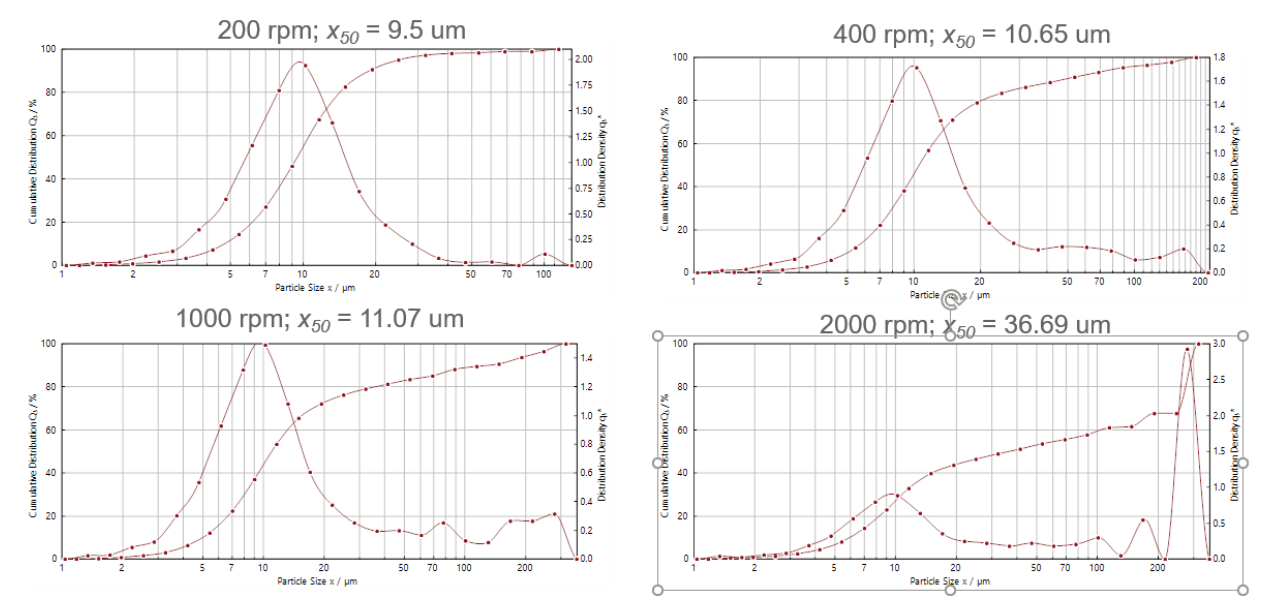


Figure 15. Four charts of particle size distribution generated by the Sympatec software for the CeO₂ powders using various stirring speeds from 200 to 2,000 rpm. It appears values between 400 and 1,000 rpm give consistent average particle size values and expected bell shape distributions.

A second round of calibration runs were performed using the NIST 1984 SRM. Like the CeO_2 , but in more detail, a series of tests were performed to determine optimal parameters before the instrumented is transferred into a contamination area fume hood for PuO_2 analysis. Part of the initial calibration of the DIA is understanding the effects of particle loading, stirring speed, and pump speed.

Table 1 shows the test matrix performed this quarter on NIST 1984 SRM. Run 10 seems to have achieved the optimal mix of parameters with an average particle size of 16.55 μ m measured. This is nearly identical to the 16.5 μ m average particle size reported in the NIST reference documentation for measurements performed with a similar DIA instrument. The ease with which this standard value could be hit bodes well for the PSA as a rapid and accurate means to quantify mass particle size data for the actinide forensics community. Additionally, the DIA captured a nearly perfect bell shape distribution with little evidence of any biases or bimodal distribution. This can be seen in Figure 16. Work is ongoing to transfer this equipment to a space capable of measuring actinide materials.

Particle Size Analyzer 19

Table 1.	Test	Matrix fo	r DIA	using	NIST	1984 SRM.

	Stirrer	Pump	Optical Density at	Optical	No of	50th
Run	Speed	Speed	Start of Run	Concentration	Particles	Percentile
1	400	50	0.04	0.02	19560	13.13
2	400	100	0.03	0.02	19395	11.72
3	400	150	0.01	0	4897	13.73
4	400	200	0.01	0	5303	14.55
5	400	250	0	0	6931	16.23
6	800	50	0.02	0.03	22998	16.14
7	800	100	0.09	0.1	45234	17.61
8	800	150	0.09	0.09	43503	17.15
9	800	200	0.1	0.1	49380	17.25
10	800	250	0.09	0.11	54104	16.55
11	1200	50	0.06	0.07	44422	16.06
12	1200	100	0.16	0.16	72187	17.21
13	1200	150	0.17	0.15	71778	18.17
14	1200	200	0.15	0.14	72999	16.31
15	1200	250	0.17	0.16	77012	17.11
16	1600	50	0.08	0.09	56352	15.9
17	1600	100	0.2	0.18	78337	18.96
18	1600	150	0.17	0.17	76275	21.41
19	1600	200	0.2	0.18	85485	18.76
20	1600	250	0.18	0.18	74285	37.2
21	2000	50	Too many bubbles			
22	2000	100	Too many bubbles			
23	2000	150	Too many bubbles			
24	2000	200	Too many bubbles			
25	2000	250	Too many bubbles			

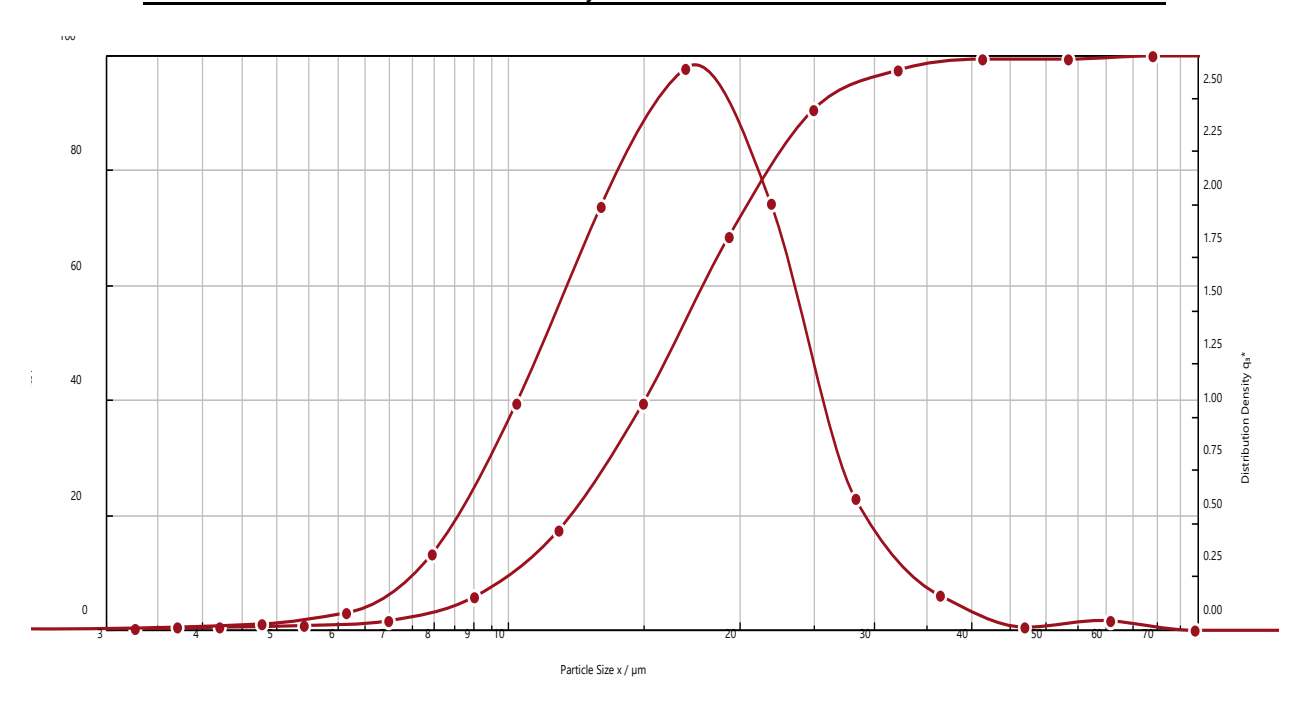


Figure 16. Optimal DIA pump speed (250) and stirrer speed (800) as determined by the shape of the distribution curve and the exact match to the average particle size listed (16.5 μ m) in the NIST 1984 SRM reference documentation.

Particle Size Analyzer 20

5.0 Atomic Force Microscopy

AFM was identified as an additional imaging method that could provide detailed topological information. The potential for AFM to provide new and unique signatures is promising, with multiple analysis modes including hardness, Young's modulus, and thermal conductivity mapping. Development of this technique for both imaging and property analysis may introduce a powerful new tool for the actinide forensics community. Initial work was performed in simple tapping imaging mode on SEM sample stubs that used the wet dispersion method utilized by the SEM and MAMA analysis.

Figure 17 shows the topography, deflection, and phase mapping of the initial imaging. One drawback to AFM is that it is more of a high-magnification method and it is not capable of imaging as many particles in a single image as SEM. With that said, the comparison of the measured height and diameter of the particles reveals some interesting features of the carbon tape mounting method. Primarily, it appears that particles are heavily recessed into the substrate. The measured portion sunk past the maximum diameter of an assumed sphere by ~20%, which coincides incredibly well with the reduction in average particle size of the SEM/MAMA analysis from both the dry and wet dispersion methods using the NIST standard (~20-25%). This can be seen in Table 2.

A proposed correction factor of 1.33 has been proposed for future SEM/MAMA analysis to correct for this baseline bias. This correction factor should be refined in the future to have weighting factors based on particle mass as it is assumed heavier particles will sink into the substrate to a greater degree than light particles. Future work is also needed to improve the mounting surface such that its sticky enough to prevent PuO₂ contamination but leads to less embedding of particles.

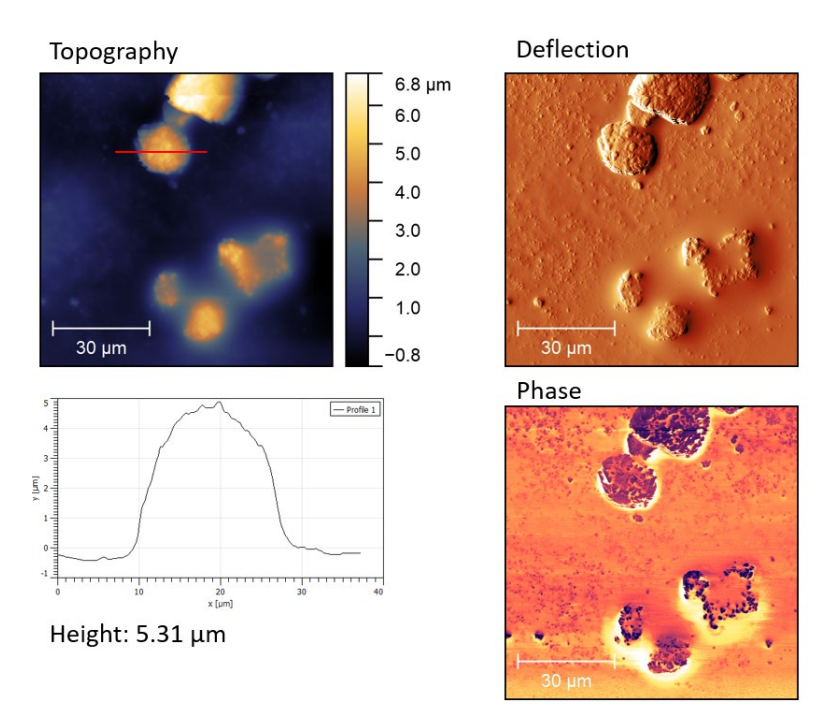


Figure 17. AFM topography, deflection, and phase imaging showing heavy recession of the NIST 1984 SRM into the carbon tape.

Table 2. AFM NIST 1984 particle recession into carbon sticky tape analysis.

Particle Dimensions	Α	В	С
Height (µm)	5.3	3.8	4.8
Equivalent disk diameter (µm)	16.6	12.5	18.4
Approx. portion sunk	68%	70%	74%

6.0 Mentorship and Expertise Development

Throughout this project, a large emphasis was placed on early career development of junior staff and students, including one early career staff scientist (Jason Lonergan), one post doc (Kyle Makovsky), and two PhD interns (Michaella Swinhart and Vitaliy Goncharov). The early career scientist developed project management skills, which included leading a team toward successful completion of a task on time and within budget. The post doc and both PhD interns received radiological worker training and expertise development that included work within radiological fume hoods and glove boxes. The junior staff scientist and post doc received training and became independent users on the SEM and PSA. All staff present received training in PSA using the MAMA software.

7.0 Future Work

With the wet dispersion method sufficiently improved utilizing heavy liquids, NIST standards, and an actinide surrogate (CeO₂), future work will involve continued refinement of the SEM/MAMA method as well as imaging and analysis of PuO₂ powders. This work will be transferred to ongoing nuclear forensics projects funded by the National Nuclear Security Administration. With confidence that a representative aliquot is now being delivered to the SEM, a second attempt will be made to discover morphological forensic signatures correlated to specific processing conditions.

The goal is to publish at least two journal articles. One article will describe the improved methodology for wet dispersion sampling and SEM imaging of actinide particles. The second article will detail forensic signatures found using SEM morphological analysis on various PuO₂ particles syntheses using different processing conditions. A second effort will be undertaken to devise a simplified morphological intragranular feature numbering system, like Tamasi, that can transform what has traditionally been qualitative analysis into something quantitative.[9]

Future Work 24

8.0 Summary

The primary goal of this project was to develop a methodology for bias correction in the particle sampling that was previously performed in the SDS. This was divided into two tasks. The first task was to develop a correction factor/formula that could be applied to existing data sets from the SDS. The second task was to enhance the sample preparation methodology such that a correction factor would not be needed in future SEM morphological analysis.

Unfortunately, a simple correction factor/formula was not generated for the 76 runs in the SDS data set. It was confirmed during early analysis on a NIST particle size standard that the original wet dispersion method resulted in a heavy bias in the MAMA PSA. Initial Stokes' setting calculations confirmed that larger/heavy particles, representing a good majority of the PuO $_2$ in the SDS, were settling at a far greater rate than previously expected, resulting in underrepresentation of particles as small as 10 μ m in diameter. This was confirmed by analysis of the NIST 1984 SRM using the SDS wet dispersion method.

A total of 3,000 particles were analyzed using MAMA software, involving ~100 separate SEM images. An average particle size of 6.1 μ m was calculated, which is ~65% smaller than the reported value for the NIST 1984 SRM (17.1 μ m). At this point, it was determined that a simple correction factor could not be applied across the board as the specific shape and size of the powders in each of the 76 runs would lead to a unique settling rate that would require a unique correction factor/formula. It was determined that this level of correction was outside the scope and budget of the project.

Fortunately, the second task was successful, and an improved sampling methodology was developed that has vastly improved the wet dispersion method to give a representative aliquot using a heavy liquid that significantly slows the settling of large particles. The accuracy of this aliquot has been verified with comparison to both the NIST 1984 SRM and use of a PSA. A total of 3,689 particles were measured across five SEM sample stubs, using three analysts, yielding an average particle size of 12.69 µm. This is more than double the average for the same powder and removed large bi-modal distributions within the data set. Although the average particle size is still ~25% lower than the 17.1 µm average reported by the NIST standard, further analysis with an AFM has indicated that particles sunk into the carbon tape. These measurements indicate that the maximum diameter of an analyzer sphere/grain could reasonably have a measured diameter that is ~20-25% less than the maximum diameter. This coincides incredibly well with the reduction in average particle size of the SEM/MAMA analysis from the NIST standard.

Improved adhesion material for future PuO_2 sampling could easily remedy the final discrepancy between the NIST standard and the current wet dispersion method. Additionally, the resulting log normal distribution that matches the NIST data set indicates there is a good potential for the future development of a correction factor for this improved sampling method. Furthermore, a statistical analysis study of note was performed by randomly sub-sampling the total NIST 1984 SRM data set from the new LST wet dispersion method, showing that random sets of only 300 particles accurately maintained the log normal distribution and mean particle size. This is highly encouraging for future SEM imaging and MAMA analysis as the time scale to fully capture important morphological trends can be reduced by hundreds of man hours.

Summary 25

Further work was performed using CeO_2 as a surrogate actinide material to test and compare the improved wet dispersion method with the PSA using controls and safety features that will be utilized for PuO_2 (i.e., glove box, fume hood, special shielding equipment). An average particle size of 11.55 μ m was calculated from analysis of 333 particles for the SEM/MAMA method compared to an average particle size of 10.89 μ m determined between the averaging of several runs and hundreds of thousands of particles by the PSA. This is further proof that the improved sampling methodology for the SEM/MAMA method can give accurate and representative aliquots of the larger bulk powder sample and additional evidence that multiple thousands of particles may not need to be analyzed in MAMA to get an accurate/representative distribution and average grain size data.

Although the focus of this study was bulk particle size statistics such as those captured in the SDS, it should be noted that the SEM is capable of additional morphological and structural characterization that is beneficial for nuclear forensics analysis. For instance, the SEMs have the added advantage of EDS analysis, allowing the distinction of PuO₂ particles from contaminants or other possible processing additives. Focused ion beam SEM microscopes are capable of cross-sectioning particles to analyze intergranular structure. SEM imaging also allows one to extend the characterization past particle outlines and to start developing a quantitative descriptive system for intragranular features.

The PSA and the automated software analysis that can capture and analyze hundreds and thousands of particles in seconds may sound like the ultimate morphological analysis tool; however, the resulting raw data from this method is only black and white pixelated outlines. This method is great for rapid particle size statistics, but it doesn't provide the depth of data and functionality that is available with a modern SEM. For instance, particle agglomeration or contamination would be impossible to segregate from the analysis. Furthermore, a robust connection between overall particle size or shape and specific processing conditions has not been confirmed to date. On the other hand, many unique surface features and crystal growth patterns are contained within the particles and present the potential for powerful processing signatures – especially when only a handful of grains are present. This data will only be available to techniques that produce high-quality, data-rich images. In addition, the automated particle analysis software is not exclusively tied to the PSA and could be adapted to SEM image analysis, further reducing the time discrepancy between the two methods.

Ultimately, both the PSA and SEM are potentially powerful tools for morphological characterization within the field of nuclear forensics, but the used of each must be chosen with care depending on the data desired and available material.

Summary 26

9.0 References

- 1. E.F. Fiock and W.H. Rodebush, *The vapor pressures and thermal properties of potassium and some alkali halides.* Journal of the American Chemical Society 1926. **48**: p. 2522.
- 2. Nuclear Forensics in Support of Inbestigations (Implementing Guide). 2015, International Atomic Energy Agency. p. 1-80.
- 3. I.J. Schwerdt, et al., *Nuclear forensic investigation of morphological signatures in the thermal decomposition of uranyl peroxide* Talanta, 2018. **176**: p. 284-292.
- 4. K.J. Moody, I.D. Hutcheon, and P.M. Grant, *Nuclear Forensic Analysis*. 2005, Boca Raton, FL: CRC Press.
- 5. Klaus Mayer, Maria Wallenius, and Z. Varga, *Nucler Forensic Science (Correlating Measurable Matieral Parameters to the History of Nuclear Material).* Chemical Reviews 2013. **113**: p. 884-900.
- 6. Z. Varga, et al., *Trends and perspectives in Nuclear Forensic Science* Trends in Analytical Chemistry 2022(146): p. 116503.
- 7. D.S. Schwartz and L. Tandon, *Unertainty in the use of MAMA software to measure particle morphological parameters from SEM imgages.* 2017: United Sates
- 8. Schwartz, D.S., *Documentation of operational protocol for the use of MAMA software.* 2016: United States
- 9. A.L. Tamasi, et al., *A lexicon for consistent description of material images for nuclear forensics* Journal of Radioanalytical and Nuclear Chemistry 2016. **307**: p. 1611-1619.

References 27

Pacific Northwest National Laboratory

902 Battelle Boulevard P.O. Box 999 Richland, WA 99354

1-888-375-PNNL (7665)

www.pnnl.gov